

## **The synthesis of W-Ni<sub>3</sub>S<sub>2</sub>/NiS nanosheets with heterostructure as high efficiency catalyst for urea oxidation**

Han Zhao<sup>a</sup>, Min Liu<sup>a</sup>, Xiaoqiang Du<sup>a\*</sup> and Xiaoshuang Zhang<sup>b</sup>

<sup>a</sup> School of Chemistry and Chemical Engineering, Shanxi Key Laboratory of High Performance Battery Materials and Devices, North University of China, Xueyuan road 3, Taiyuan 030051, People's Republic of China. E-mail: duxq16@nuc.edu.cn

<sup>b</sup> School of Environment and Safety Engineering, North University of China, Xueyuan road 3, Taiyuan 030051, People's Republic of China.

### **Chemicals and reagents**

The nickel foam (NF, thickness 1.0 mm) was obtained by Kunshan Guangjiayuan New Material Co., Ltd; The thioacetamide (TAA, CH<sub>3</sub>CSNH<sub>2</sub>) from Sarn Chemical Technology (Shanghai) Co., Ltd; The sodium tungstate (Na<sub>2</sub>WO<sub>4</sub>) from Tianjin Sinopharm Chemical Reagent Factory.; Polyvinylpyrrolidone (PVP) from Tianjin Guangfu Fine Chemical Research Institute; potassium hydroxide (KOH) from Tianjin Damao Chemical Reagent Factory; Urea (CO(NH<sub>2</sub>)<sub>2</sub>) from Tianjin Damao Chemical Reagent Factory; Concentrated hydrochloric acid (HCl, 12 mol/L) was bought from Chengdu Cologne Chemical Co., LTD.

### **DFT computation details:**

The DFT calculations were performed using the Cambridge Sequential Total Energy Package (CASTEP) with the plane-wave pseudo-potential method. The geometrical structures of the (220) plane of W-Ni<sub>3</sub>S<sub>2</sub>, and the (110) plane of NiS was optimized by the generalized gradient approximation (GGA) methods. The Revised Perdew-Burke-Ernzerh of (RPBE) functional was used to treat the electron exchange correlation interactions. A Monkhorst Pack grid k-points of 6\*8\*1 and 5\*6\*1 of W-Ni<sub>3</sub>S<sub>2</sub> and NiS, a plane-wave basis set cut-off energy of 500 eV were used for integration of the Brillouin zone. The structures were optimized for energy and force convergence set at 0.05 eV/Å and 2.0×10<sup>-5</sup> eV, respectively.

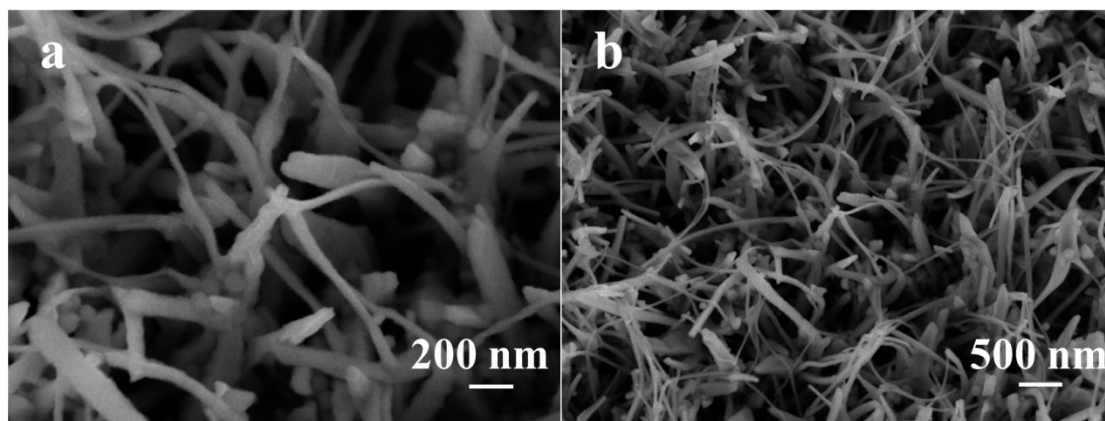


Fig.S1 SEM images of W-Ni<sub>3</sub>S<sub>2</sub>.

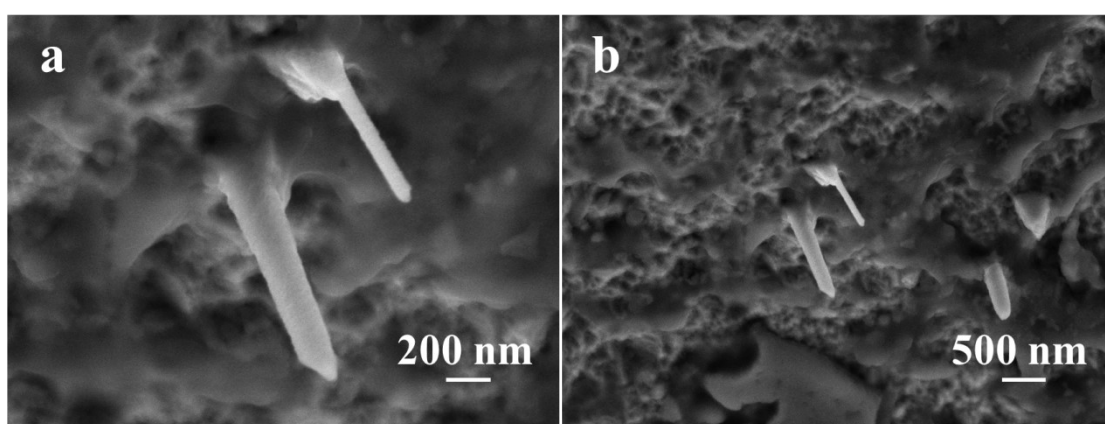


Fig.S2 SEM images of Ni<sub>3</sub>S<sub>2</sub>.

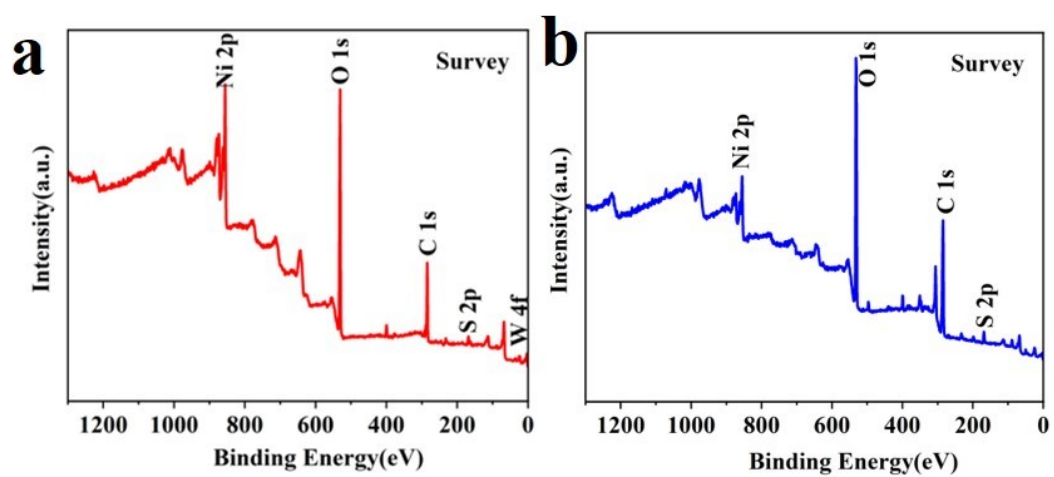


Fig.S3 Survey of a) W-Ni<sub>3</sub>S<sub>2</sub>/NiS, b) Ni<sub>3</sub>S<sub>2</sub>.

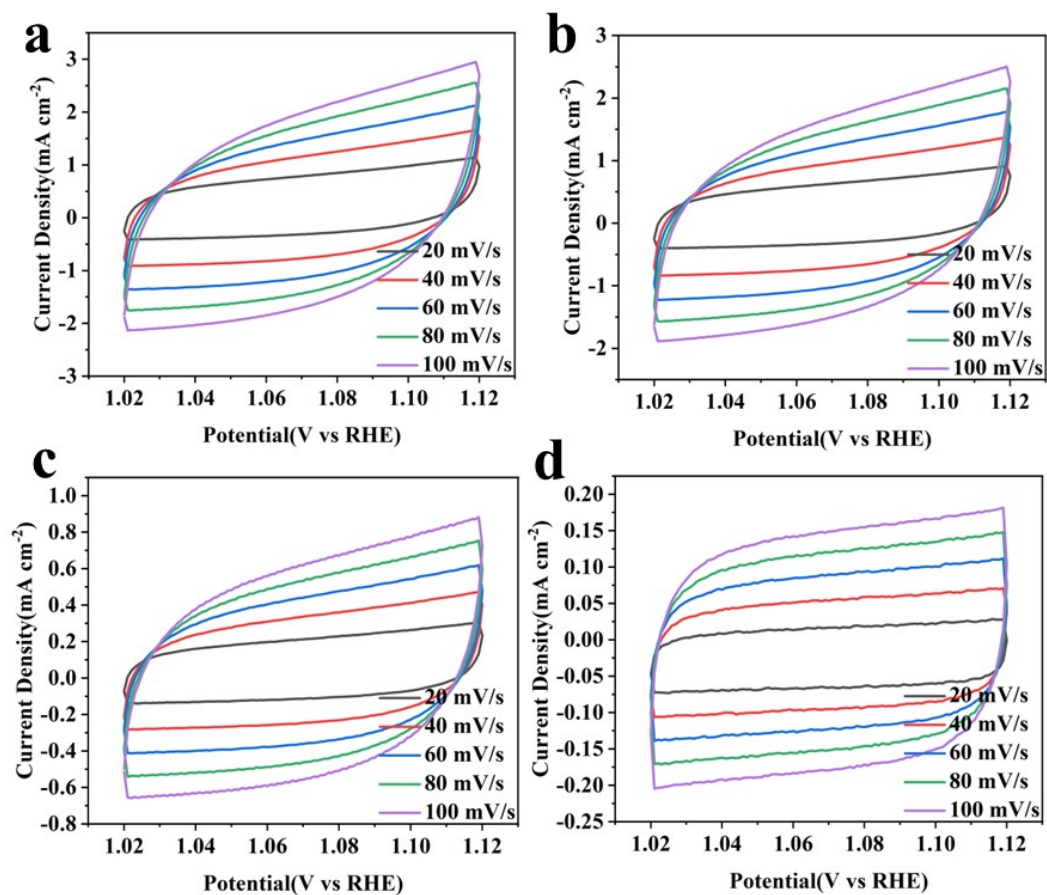


Fig.S4 CV plots of a) W-Ni<sub>3</sub>S<sub>2</sub>/NiS, b) W-Ni<sub>3</sub>S<sub>2</sub>, c) Ni<sub>3</sub>S<sub>2</sub>, d) NF at different scan rates.

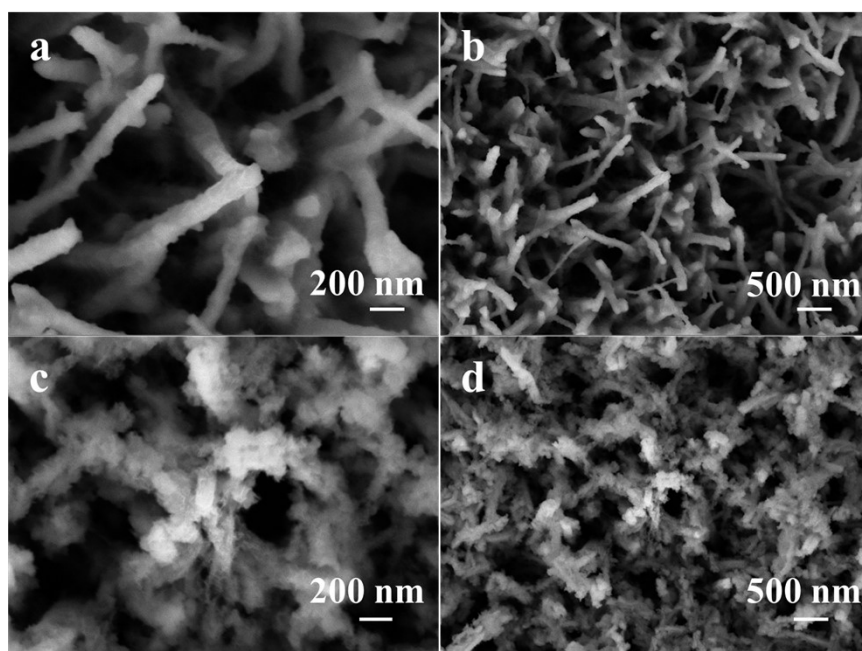


Fig.S5 SEM images of W-Ni<sub>3</sub>S<sub>2</sub>/NiS before(a-b)and after(c-d)stability test.

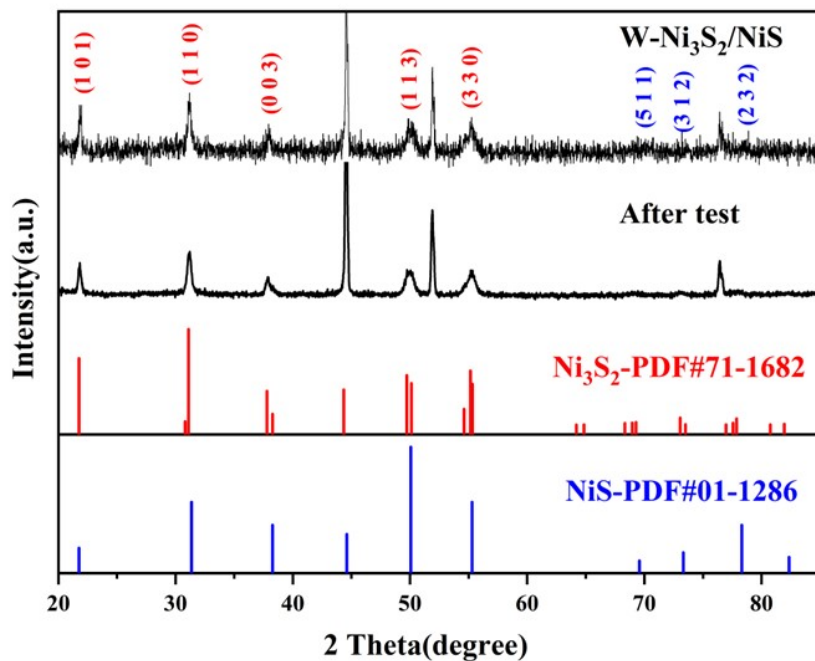


Fig.S6 XRD patterns of W-Ni<sub>3</sub>S<sub>2</sub>/NiS before and after stability test.

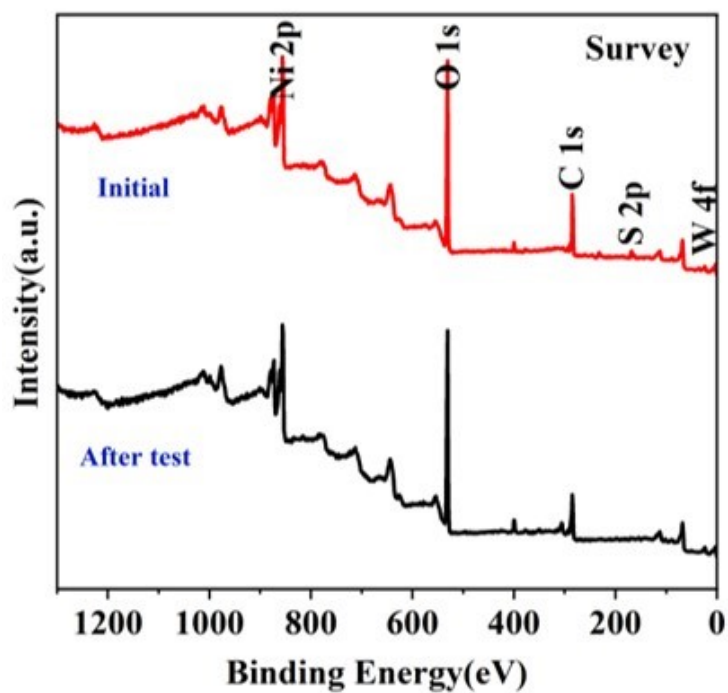


Fig.S7 XPS of W-Ni<sub>3</sub>S<sub>2</sub>/NiS before and after stability test.

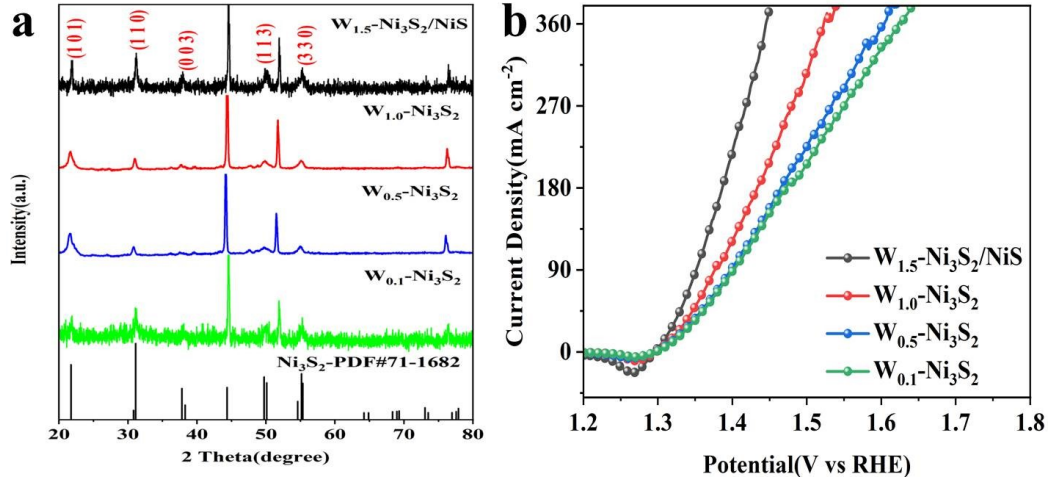


Fig. S8 XRD (a) and UOR (b) performance of as prepared materials.

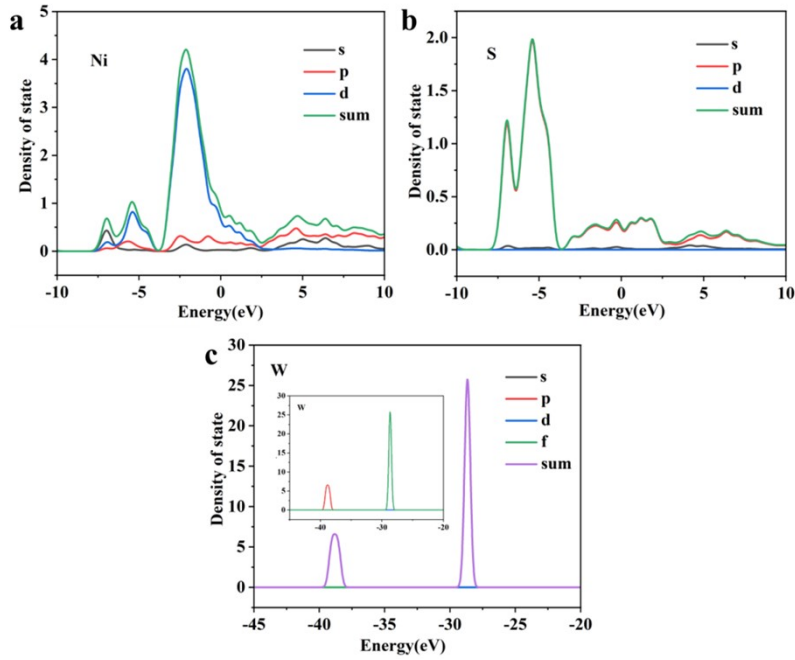


Fig. S9 Density of states for W-Ni<sub>3</sub>S<sub>2</sub>, (a) Ni, (b) S and (c) W.

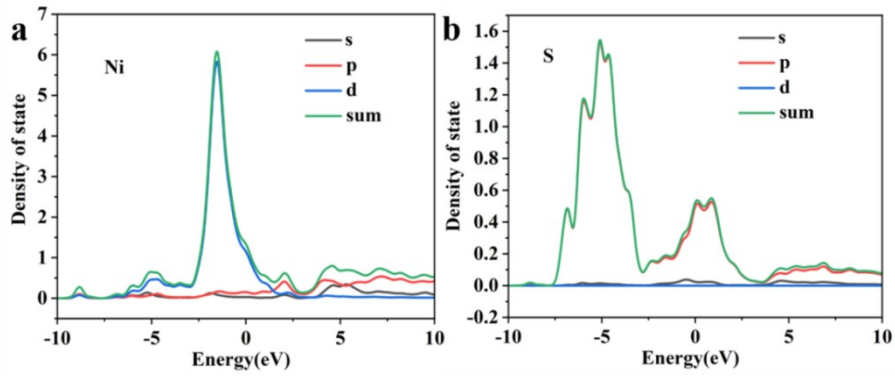
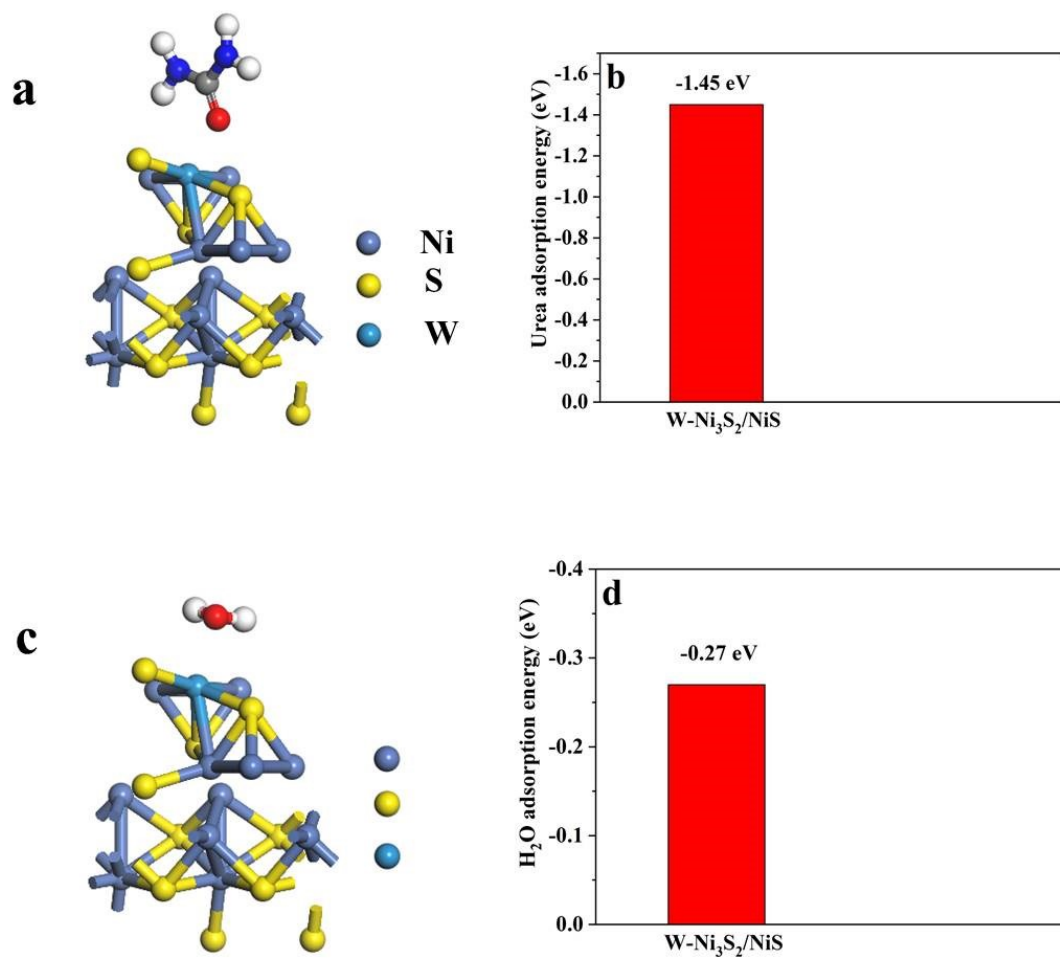


Fig. S10 Density of states for NiS, (a) Ni and (b) S.



**Fig. S11** The ball-and-stick model of urea adsorbed on (a) W-Ni<sub>3</sub>S<sub>2</sub>/NiS and (b) Urea adsorption energy; the ball-and-stick model of H<sub>2</sub>O adsorbed on (c) W-Ni<sub>3</sub>S<sub>2</sub>/NiS and (d) H<sub>2</sub>O adsorption energy.

**Table S1** Comparison of charge transfer resistance (R<sub>2</sub>) values of all samples in alkaline solution (UOR).

catalyst	R <sub>2</sub> (Ω)
<b>W-Ni<sub>3</sub>S<sub>2</sub>/NiS</b>	<b>0.895</b>
W-Ni <sub>3</sub> S <sub>2</sub>	1.088
Ni <sub>3</sub> S <sub>2</sub>	1.304
NF	5.584*10 <sup>16</sup>

**Table S2** Comparisons of UOR activity of non-noble-metal electrocatalysts.

catalysts	Electrolytes	Potential(V)	Reference
<b>W-Ni<sub>3</sub>S<sub>2</sub>/NiS</b>	<b>1M KOH+0.5M urea</b>	<b>1.309 V</b>	<b>This work</b>
Ni <sub>3</sub> S <sub>2</sub> @MoS <sub>2</sub> CS	1M KOH+0.5M urea	1.336 V	1
Mn-NiS <sub>x</sub> /NiO/Ni <sub>3</sub> N	1M KOH+0.5M urea	1.35 V	2
FeCo-LDH	1M KOH+0.5M urea	1.328 V	3
Ce-Ni <sub>3</sub> N@CC	1M KOH+0.5M urea	1.31 V	4
FeMn-PS	1M KOH+0.33M urea	1.33 V	5
O-NiMoP/NF	1M KOH+0.5M urea	1.31 V	6
Mn-Ni <sub>3</sub> S <sub>2</sub> /NF	1M KOH+0.5M urea	1.30 V	7
Mo-doped Ni <sub>3</sub> S <sub>2</sub>	1M KOH+0.3M urea	1.33 V	8
MOF-Ni@MOF-Fe-S	1M KOH+0.5M urea	1.347 V	9
VOOH-Ni	1M KOH+0.33M urea	1.356 V	10

## References

1. Qun, L.; Botao, Y.; Bowen, Z.; Yuanpeng, J.; Haodong, X.; Yongshuai, X.; Yunfa, D.; Zhezhi, L.; Yuanpeng, L.; Liang, Q.; Rui, K.; Chunhui, Y.; Jiecai, H.; Weidong, H., Bi-functional Ni<sub>3</sub>S<sub>2</sub>@MoS<sub>2</sub> heterostructure with strong built-in field as highly-efficient electrolytic catalyst. *J. Electroanal. Chem.* **2023**, *931*, 117185.
2. Peng, Y.; Yanyan, S.; Caiyun, L.; Rongzhan, L.; Jiankun, S., Heterostructured Mn-doped NiS<sub>x</sub>/NiO/Ni<sub>3</sub>N nanoplate arrays as bifunctional electrocatalysts for energy-saving hydrogen production and urea degradation. *Appl. Surf. Sci.* **2023**, *619*, 156789.
3. Gong, Y.; Zhao, H.; Ye, D.; Duan, H.; Tang, Y.; He, T.; Shah, L. A.; Zhang, J., High efficiency UOR electrocatalyst based on crossed nanosheet structured FeCo-LDH for hydrogen production. *Appl. Catal., A.* **2022**, *643*, 118745.
4. Li, M.; Wu, X.; Liu, K.; Zhang, Y.; Jiang, X.; Sun, D.; Tang, Y.; Huang, K.; Fu, G., Nitrogen vacancies enriched Ce-doped Ni<sub>3</sub>N hierarchical nanosheets triggering highly-efficient urea oxidation reaction in urea-assisted energy-saving electrolysis. *J. Energy Chem.* **2022**, *69*, 506-515.

5. Meng, X.-y.; Wang, M.; Zhang, Y.; Li, Z.; Ding, X.; Zhang, W.; Li, C.; Li, Z., Superimposed OER and UOR performances by the interaction of each component in an Fe-Mn electrocatalyst. *Dalton Trans.* **2022**, 51 (43), 16605-16611.
6. Jiang, H.; Sun, M.; Wu, S.; Huang, B.; Lee, C.-S.; Zhang, W., Oxygen-Incorporated NiMoP Nanotube Arrays as Efficient Bifunctional Electrocatalysts For Urea-Assisted Energy-Saving Hydrogen Production in Alkaline Electrolyte. *Adv. Funct. Mater.* **2021**, 31 (43), 2104951.
7. Yang, H.; Yuan, M.; Sun, Z.; Wang, D.; Lin, L.; Li, H.; Sun, G., In Situ Construction of a Mn<sup>2+</sup>-Doped Ni<sub>3</sub>S<sub>2</sub> Electrode with Highly Enhanced Urea Oxidation Reaction Performance. *ACS Sustainable Chem. Eng.* **2020**, 8348–8355.
8. Xu, H.; Liao, Y.; Gao, Z.; Qing, Y.; Wu, Y.; Xia, L., A branch-like Mo-doped Ni<sub>3</sub>S<sub>2</sub> nanoforest as a high-efficiency and durable catalyst for overall urea electrolysis. *J. Mater. Chem. A* **2021**, 9 (6), 3418-3426.
9. Xu, H.; Ye, K.; Zhu, K.; Yin, J.; Yan, J.; Wang, G.; Cao, D., Efficient bifunctional catalysts synthesized from three-dimensional Ni/Fe bimetallic organic frameworks for overall urea electrolysis. *Dalton Trans.* **2020**, 49 (17), 5646-5652.
10. Wei, D.; Tang, W.; Ma, N.; Wang, Y., Ni-doped VOOH as an efficient electrocatalyst for urea oxidation. *Mater. Lett.* **2021**, 291, 129593.